

# Artifacts of Titanium, Zirconium, and Binary Titanium-Zirconium Abutments in Compute Tomography, Cone Beam Computed Tomography, and Magnetic Resonance Imaging

Hoorieh Bashizadeh Fakhar<sup>1</sup>, Hashem Sharifian<sup>2</sup>, Mahdi Niknami<sup>1</sup>,  
Mahboobeh Iranmanesh<sup>3</sup>

<sup>1</sup>Department of Dentomaxillofacial Radiology, School of Dentistry, Tehran University of Medical Sciences

<sup>2</sup>Department of Radiology, School of Medicine, Tehran University of Medical Sciences

<sup>3</sup>Department of Dentomaxillofacial Radiology, School of Dentistry, Rafsanjan University of Medical Sciences

*Received 10 October 2019 and Accepted 14 December 2019*

## Abstract

**Aim:** The aim of this in vitro study was to evaluate imaging artifacts induced by titanium, zirconium, and titanium-zirconium abutments in computed tomography (CT), cone-beam computed tomography (CBCT), and magnetic resonance imaging (MRI) modalities.

**Methods:** A 4×8-mm titanium fixture was inserted in a dry human mandible. Titanium, zirconium, and titanium-zirconium abutments measuring 10.5 mm in height were located on the fixture one by one. Each abutment was scanned four times by each imaging modality. The gray value of the images was evaluated in four determined regions adjacent to distal, mesial, buccal, and lingual aspects of the implant as the region of interest (ROI) by two observers using the Image J software. Gray value differences ( $\Delta$ GVs) between the control (i.e., fixture without abutment) and case (i.e., fixture and each type of abutment) images were calculated. Data analysis was performed by the analysis of variance and post hoc tests.

**Results:** In the CBCT,  $\Delta$ GV was significantly higher in zirconium-titanium images, compared with that in images with titanium abutments ( $P \leq 0.05$ ). In the distal, mesial, and buccal aspects of ROI in CT, the  $\Delta$ GV was higher in zirconium images, compared with titanium abutments. In the MRI,  $\Delta$ GV for zirconium was lower than those for titanium-zirconium and titanium samples, respectively. Furthermore, no significant differences in  $\Delta$ GV were seen between T1 and T2 protocols, for all samples. **Conclusion:** In MRI, image artifacts are the least around zirconium abutments, while in CT and CBCT, titanium abutments produced the least amount of artifacts.

**Keywords:** Artifact, Implant, Titanium, Titanium-zirconium, Zirconium, CT, CBCT, MRI

-----  
BashizadehFakhar H, Sharifian H, Niknami M, Iranmanesh M. Artifacts of Titanium, Zirconium, and Binary Titanium-Zirconium Abutments in Compute Tomography, Cone Beam Computed Tomography, and Magnetic Resonance Imaging . J Dent Mater Tech 2020; 9(1): 230. 234

## Introduction

Currently, X-ray-based three-dimensional imaging is a routine part of many medical and dental examinations. Some patients may have dental implants which can dramatically reduce image quality by beam hardening artifacts (1-3). Beam hardening is a phenomenon caused by a selective attenuation of lower energy photons in objects with a large atomic number (4). Dental implants may also distort the magnetic field and result in susceptibility artifacts in magnetic resonance images (2, 5, 6). Recently, metal-free zirconia dental implants have been introduced. They have a natural and tooth-colored appearance, with higher biocompatibility and lower allergic effects (7, 8). The purpose of this study was the in vitro assessment of titanium (Ti), titanium-zirconium (Ti-ZrO<sub>2</sub>), and zirconium (ZrO<sub>2</sub>) abutment artifacts in computed tomography (CT), cone-beam computed tomography (CBCT), and magnetic resonance imaging (MRI) modalities. The results of this study may cause potential improvements in dental implant manufacturing with the target of artifact reduction in medical and dental images (9).

## Materials and Methods

In the present study, a single implant was placed in a dry human mandible in the first premolar area as the control group. The implant was 8 mm in length and 3.5 mm in diameter. The Ti (Leader Italia, 10.5 mm), Ti-ZrO<sub>2</sub> (laboratory-made, 10.4 mm), and ZrO<sub>2</sub> abutments (Leader Italia, 10.4 mm) were attached to the implant one by one. Mandible was placed in a 20×8-cm plastic water container with 3-mm wall thickness to mimic soft tissue attenuating characteristics. An acrylic tripod was designed to stabilize the mandible inside the container (Figure 1).

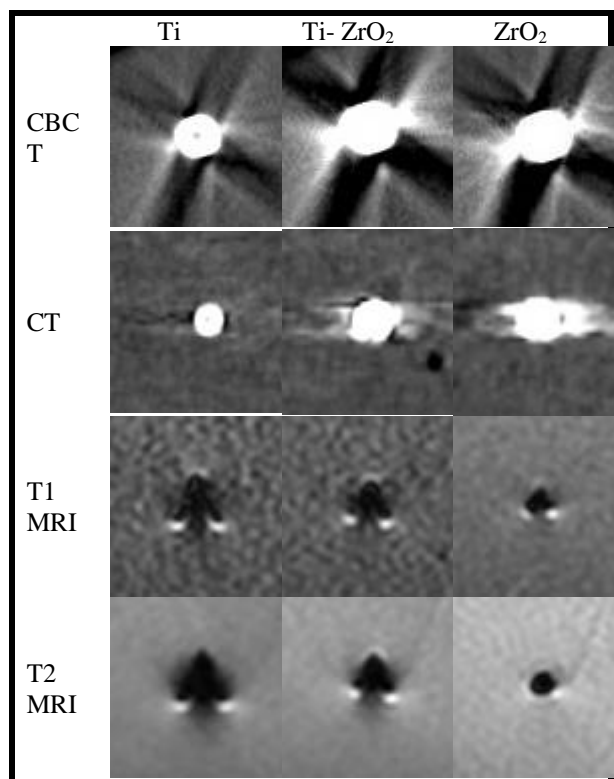


**Fig.1.** Artifacts around titanium, zirconium and binary titanium- zirconium abutments in different imaging modalities

The MRI images were acquired by a 3T MRI scanner (Siemens, Berlin, Germany). The imaging protocol consisted of axial T1 weighted images by a TE of 11.7 ms and a TR of 600 ms with 1-mm slice thickness, 192×192 matrix and 18×16.2-cm field of view. The T2 weighted images were also acquired by a TE of 60.9 ms and a TR of 2500 ms with the same slice thickness, matrix, and field of view. A 20-channel head coil was utilized in all MRI procedures.

The CT images were acquired by the Somatom Sensation 16 Slice (Siemens, Berlin, Germany) with 110 kVp, 20 mAs, 512×512 matrix, 0.33-pixel spacing, and

1-mm slice thickness. The CBCT images were prepared by the Alphard Vega 3030 (Asahi Roentgen Ind., Co. Ltd, Kyoto, Japan). Exposure parameters were 80 kVp, 5 mA, 10×10 cm field of view, and 17-sec exposure time. The minimum voxel size was chosen as 0.2 mm.

The case and control groups were scanned four times by each modality. ImageJ software (National Institute of Health, Bethesda a, MD, USA) was used to evaluate the images. The evaluation was performed on axial images at the level of the implant, near the alveolar crest for case and control groups. The region of interest (ROI) was considered as four circular areas consisting of 10×10 pixels in the buccal, lingual, mesial, and distal aspects of

The abutment (Figure 2). The mean gray value (GV) was measured for each region.

Observers reassessed each image after 2 weeks. Pearson correlation showed high inter- and intra-observer agreements. The KS test was performed on the first step observation data for analyzing the normal distribution. Due to the high level of agreement between the observers, data analysis was performed based on the mean values of two observers. In addition, the mean gray value of each ROI in each case was subtracted from the mean gray value of the same ROI in the control sample ( $\Delta$ GV). The data were analyzed in SPSS, version 22. (SPSS Inc., Chicago, IL, USA) considering a 95% confidence interval.

The intraclass Pearson's correlation coefficient was used to determine the inter-observer agreement and intra-observer reliability. One-way ANOVA and Tuckey's post hoc test were used for comparisons. A P-value less than 0.05 was considered statistically significant.

## Results

In this study,  $\Delta$ GV was evaluated around the implant with three different types of abutments in four regions, namely buccal, lingual, mesial, and distal, for three different types of images, including CT, MRI, and CBCT. Considering the high inter-observer agreement ( $P < 0.05$ ), the results were presented based on the average of the values measured by the two observers.

As Table I shows, in all regions of CBCT images, the highest  $\Delta$ GV is due to Ti-ZrO<sub>2</sub> abutments, compared to the other types of abutments ( $P \leq 0.05$ ). Furthermore, in CBCT,  $\Delta$ GV for all types of abutments was significantly higher in the mesial and distal aspects as compared to those in buccal and lingual regions ( $P \leq 0.05$ ). Among all imaging modalities, CBCT produced the most artifacts ( $P \leq 0.05$ ).

**Table I.** Gray value differences between the control and case images ( $\Delta$ GV) around different abutments in cone-beam computed tomography ( $P \leq 0.05$ )

	Mesial	Distal	Buccal	Lingual
TiZrO <sub>2</sub> (n=8)	138.53±0.95	136.49±1.73	-39.75±0.69	-21.19±1.43
Ti (n=8)	43.29±9.10	48.76±13.72	-39.57±1.84	-7.11±7.40
ZrO <sub>2</sub> (n=8)	124.08±3.18	127.46±3.08	-39.48±1.85	-9.46±10.57

According to Table II, in all regions of CT images, the highest  $\Delta$ GV is due to ZrO<sub>2</sub> abutments, compared to the other types of abutments ( $P \leq 0.05$ ). The  $\Delta$ GV in CT for all types of abutments was also significantly higher in the mesial and distal aspects than in the buccal and lingual regions ( $P \leq 0.05$ ). Data analysis showed almost

similar results in T1 and T2 protocols in MRI for the different types of abutments. Considering all regions in MRI images, the highest  $\Delta$ GV was due to Ti abutments, compared to the other types of abutments ( $P \leq 0.05$ ; Tables III and IV).

**Table II.** Gray value differences between the control and case images ( $\Delta$ GV) around an abutment in computed tomography ( $P \leq 0.05$ ).

	Mesial	Distal	Buccal	Lingual
TiZrO <sub>2</sub> (n=8)	74.50±8.85 <sup>b</sup>	42.31±7.97	4.61±2.16	-1.85±2.80
Ti (n=8)	11.58±4.37	1.66±4.35	0.95±1.50	-1.26±0.93
ZrO <sub>2</sub> (n=8)	105.83±1.14	47.43±3.25	6.24±0.91	-4.45±2.50

**Table III.** Gray value differences between the control and case images ( $\Delta$ GV) around an abutment in T1 magnetic resonance imaging ( $P \leq 0.05$ )

	Mesial	Distal	Buccal	Lingual
TiZrO <sub>2</sub> (n=8)	-20.58±3.35	-40.03±4.22	-21.26±4.52	-22.24±4.36
Ti (n=8)	-33.45±4.97	-50.11±3.42	-29.56±3.74	-30.04±5.55
ZrO <sub>2</sub> (n=8)	-4.64±0.89	-9.65±1.08	-6.59±1.44	-6.57±1.95

**Table IV.** Gray value differences between the control and case images ( $\Delta$ GV) around an abutment in T2 magnetic resonance imaging ( $P \leq 0.05$ )

	Mesial	Distal	Buccal	Lingual
TiZrO <sub>2</sub> (n=8)	-24.72±4.00	-61.44±5.01	-35.77±4.37	-49.71±3.63
Ti (n=8)	-41.98±3.49	-85.25±3.56	-48.45±1.58	-70.55±6.71

ZrO <sub>2</sub>	-10.39±1.23	-16.50±1.74	-10.69±1.64	-10.32±1.55
(n=8)				

## Discussion

This in vitro study evaluated the artifacts around different abutments in three imaging modalities by GV analysis. In CBCT, Ti-ZrO<sub>2</sub> abutment caused the most pronounced artifacts. In CT, the ZrO<sub>2</sub> and Ti-ZrO<sub>2</sub> abutments produced the highest amount of artifacts, respectively. According to the literature, metal artifacts in CT and CBCT are the outcomes of radiopacity which indicates the X-ray inability to pass through these materials (10). Pekkan et al. (11) investigated the radiopacity of ceramic, metal, and dental tissue by a densitometer. They reported the radiopacity of ZrO<sub>2</sub> to be twice as that of Ti. The results showed the artifacts in CBCT were more than those in CT. Routinely, the field of view that is selected in routine CBCT examinations is smaller than a whole head size. When some parts of a relatively large structure remain out of the field of view in CBCT, artifacts are increased. This could be one of the reasons for substantial artifacts in CBCT in comparison to those in CT (15).

On the other hand, Langlade et al. (10) stated that different factors, such as dimension, form, density, and physical characteristics, affect the radiodensity of the objects. One of the main factors that affect radiopacity is the atomic number. Therefore, it would be obvious that ZrO<sub>2</sub> (ZZr=40, ZO=8) causes more artifacts than Ti (ZTi=22) in CT and CBCT. However, Snachopuchades et al. evaluated the artifacts of different types and different sizes of implants and proved that Zr implants produced more artifacts in CT and CBCT images. They also observed that parallel with Smeets et al. the larger implants caused more artifacts (2, 12). Furthermore, this study showed that Zr-Ti and Zr abutments produced fewer artifacts than Ti abutments in MRI. These observations are in line with those of Smeets et al. (2, 12). In their study, 15% Zr substitution in Zr-Ti abutments did not reduce the artifacts significantly (2). Duttenhoefer et al. (13) also showed MRI to be the best imaging technique for Zr implants. Matsuura et al. (14) evaluated the artifacts in neurosurgical implants in MRI. They concluded that Zr implants produce the least amount of artifacts in MRI 3T. Their study showed that the alumina ingredient of Zr increased the artifact diameter. The crystal structure, as well as the variation in particle size in alumina and Zr, seems to be in charge. They also reported minor differences between pure Ti and Ti alloys. The results of the present study may contribute to the

clinicians in implant selection for their patients to avoid potential problems in upcoming imaging procedures.

Given that this study was performed in vitro, it was not possible to reconstruct all clinical conditions. In future studies, it is recommended to evaluate the artefact of other common metallic and nonmetallic dental materials in dentistry.

## Conclusion:

It has been observed that the Ti Abutments in CT and CBCT produce less artifacts than the other abutments. On the other hand, in MRI, zirconia abutments produce less artifacts than titanium abutments.

**Conflict of Interests:** Not Declared.

## References

1. Detterbeck A, Hofmeister M, Hofmann E, Haddad D, Weber D, Holzing A, et al. MRI vs. CT for orthodontic applications: comparison of two MRI protocols and three CT (multislice, cone-beam, industrial) technologies. *J Orofac Orthop.* 2016;77(4):251-261.
2. Smeets R, Schollchen M, Gauer T, Aarabi G, Assaf AT, Rendenbach C, et al. Artefacts in multimodal imaging of titanium, zirconium and binary titanium-zirconium alloy dental implants: an in vitro study. *Dentomaxillofac Radiol.* 2017;46(2):20160267.
3. Esmaeili F, Johari M, Haddadi P. Beam hardening artifacts by dental implants: Comparison of cone-beam and 64-slice computed tomography scanners. *Dent Res J (Isfahan).* 2013;10(3):376-381.
4. Schulze RK, Berndt D, d'Hoedt B. On cone-beam computed tomography artifacts induced by titanium implants. *Clin Oral Implants Res.* 2010;21(1):100-107.
5. Hong HR, Jin S, Koo HJ, Roh JL, Kim JS, Cho KJ, et al. Clinical values of (18) F-FDG PET/CT in oral cavity cancer with dental artifacts on CT or MRI. *J Surg Oncol.* 2014;110(6):696-701.
6. Klinkle T, Daboul A, Maron J, Gredes T, Puls R, Jaghsi A, et al. Artifacts in magnetic resonance imaging and computed tomography caused by dental materials. *PLoS One.* 2012;7(2):e31766.

7. Ozkurt Z, Kazazoglu E. Zirconia dental implants: a literature review. *J Oral Implantol.* 2011;37(3):367-376.
8. Scarano A, Piattelli M, Caputi S, Favero GA, Piattelli A. Bacterial adhesion on commercially pure titanium and zirconium oxide disks: an in vivo human study. *J Periodontol.* 2004;75(2):292-296.
9. White SC, Pharoah MJ. *Oral radiology, Principles and interpretation.* 7<sup>th</sup> Ed Mosby, 2014.
10. Nagarajappa AK, Dwivedi N, Tiwari R. Artifacts: The downturn of CBCT image. *J Int Soc Prev Community Dent.* 2015;5(6):440-445.
11. Pekkan G, Pekkan K, Hatipoglu MG, Tuna SH. Comparative radiopacity of ceramics and metals with human and bovine dental tissues. *J Prosthet Dent.* 2011;106(2):109-117.
12. Sancho-Puchades M, Hammerle CH, Benic GI. In vitro assessment of artifacts induced by titanium, titanium-zirconium and zirconium dioxide implants in cone-beam computed tomography. *Clin Oral Implants Res.* 2015;26(10):1222-1228.
13. Duttonhoefer F, Mertens ME, Vizkelety J, Gremse F, Stadelmann VA, Sauerbier S. Magnetic resonance imaging in zirconia-based dental implantology. *Clin Oral Implants Res.* 2015;26(10):1195-1202.
14. Matsuura H, Inoue T, Konno H, Sasaki M, Ogasawara K, Ogawa A. Quantification of susceptibility artifacts produced on high-field magnetic resonance images by various biomaterials used for neurosurgical implants. Technical note. *J Neurosurg.* 2002;97(6):1472-1475.
15. Bryant JA, Drage NA, Richmond S. Study of the scan uniformity from an i-CAT cone beam computed tomography dental imaging system. *Dentomaxillofac Radiol.* 2008; 37(7):365-374.

**Corresponding Author**

Mahdi Niknami

Department of Dentomaxillofacial Radiology, School of Dentistry, Tehran University of Medical Sciences  
North Kargar st, Tehran Dental School, Tehran, Iran

Tell: 051 38829501

Email: niknami81@yahoo.com